

Design of High Output Broadband Piezoelectric Energy Harvester with Double Tapered Cavity Beam

Ramalingam Usharani¹, Gandhi Uma^{2#}, and Mangalanathan Umapathy²

¹ Department of Instrumentation and Control Engineering, Seshasayee Institute of Technology, Tiruchirappalli 620010, Tamilnadu, India

² Department of Instrumentation and Control Engineering, National Institute of Technology, Tiruchirappalli 620015, Tamilnadu, India

Corresponding Author / Email: guma@nitt.edu, TEL: +91-4312503359, FAX: +91-4312500133

KEYWORDS: Broadband, Energy harvester, Piezoelectric, Resonance, Vibration

Design of piezoelectric energy harvester for a wide operating frequency range is a challenging problem and is currently being investigated by many researchers. Widening the operating frequency is required, as the energy is harvested from ambient source of vibration which consists of spectrum of frequency. This paper presents a technique to increase the operating frequency range and to enhance the amplitude of the generated voltage in the operating frequency range. The wider operating frequency range is achieved by designing a harvester using propped cantilever beam with variable overhang and the amplitude of the generated voltage is enhanced by introducing a double tapered cavity. The proposed piezoelectric energy harvester is modeled analytically using Euler Bernoulli beam theory. The results from the modeling and analysis reveal that the maximum voltage is generated from the energy harvester designed with the double tapered cavity having the taper angle of $\alpha = 2.25^\circ$. Hence the experimental investigations are carried out with this energy harvester and the generated voltage measured is in close agreement with the results obtained from the model. The simulation and experimental results presented in this paper demonstrate that the proposed harvester design not only widens the operating frequency range but also it enhances the amplitude of the generated voltage in large extent.

Manuscript received: January 24, 2016 / Revised: August 17, 2016 / Accepted: August 18, 2016

1. Introduction

Energy harvesting from ambient vibrations in the environment using piezoelectric materials has been the area of interest for many researchers in the last decade. Future low power electronic devices, wireless sensors, machine condition monitoring sensors, implantable devices etc will harvest energy from their operating environment for their operation. Review of energy harvesting from mechanical vibrations using piezoelectric materials and the harvesting devices developed are reported in Refs. 1-3. The ambient vibration in the environment in general consists of a spectrum of frequency. Hence the application of energy harvesters designed to operate at a particular frequency is highly limited as it produces maximum output only at that frequency. To overcome this limitation, energy harvesters are designed to widen the operating frequency in recent years.^{4,5}

A broadband energy harvester with multiple cantilevers with different length and tip masses attached to a common base was suggested in Ref. 6. The operating frequency range was broadened by connecting multiple piezoelectric bimorphs with different aspect ratios.⁷ A broadband vibration based energy harvester with a double mass cantilever was

proposed in Ref. 8. An L shaped beam mass structure having the first two natural frequencies close to each other for broad band energy harvesting was designed in Ref. 9. Wide band piezoelectric power harvester using two piezoelectric beams with resonant frequencies close to each other when connected electrically and elastically by an end spring was demonstrated in Ref. 10. A piezoelectric energy harvester which consists of two beams with the magnets attached to the free ends was proposed in Ref. 11. A piezoelectric energy harvester with a multimode dynamic magnifier was proposed in Ref. 12 to increase the bandwidth. To provide larger bandwidth as compared to the conventional single degree of freedom and two degree of freedom piezoelectric energy harvesters, a two degree of freedom cutout cantilever piezoelectric energy harvester was proposed in Ref. 13.

A tunable dual cantilever piezoelectric energy scavenger which provides mechanically variable and adjustable tip stiffness and axial load was reported in Ref. 14. A broad band piezoelectric energy harvester using a simply supported piezoelectric beam with a dynamic compressive loading via non linear magnetic force was reported in Ref. 15. A broadband energy harvester using multi resonant beams was developed, investigated in Ref. 16.

A two degree of system that uses both rotational and translational displacements is proposed in Ref. 17, which exhibits double power peaks and an increased frequency bandwidth. Broadband Energy harvester designed using flexible frame with interdigital structure, modeling and characterization of piezomagnetoelastic broadband energy harvester and a nonlinear vibration energy harvester which combines a nonlinear bistable broadband piezoelectric cantilever are reported in Refs. 18-20. A method to increase the harvested power by splitting of piezoelectric cantilever beams of smaller width is reported in Ref. 21. The structures for harvesting energy using piezoelectric, suggested by the researchers are complex in design, as it incorporates or involves additional components such as mass, additional beams, altering the shape etc., for achieving wide operating frequency range (broadband) of the energy harvester. In this paper, a piezoelectric energy harvester using propped cantilever beam having double tapered cavity with variable overhang is proposed. In the proposed design, the broad operating frequency is obtained by means of placing a movable support along the length of the cantilever beam and higher output voltage is generated by introducing a double tapered cavity in the beam. The use of propped cantilever beam with variable overhang length to broaden the frequency band of piezoelectric energy harvester reported in this paper is first of its kind. In continuation of this, a double tapered cavity is introduced in the propped cantilever beam with overhang to enhance the generated voltage in the broadened frequency range. Simple mechanical means can be devised to move the support with ambient vibration frequency variation without additional power requirement.”

2. Energy Harvester Structure and Its Description

The structure for broadening the bandwidth of the piezoelectric energy harvester using propped cantilever beam having double tapered cavity with variable overhang length is shown in Fig. 1. The resonant frequency of the energy harvester can be tuned by varying the overhang length. A double tapered cavity with the tapering angle α is shaped at a distance of L_1 from the fixed end and at a distance of t_1 from the bottom surface of the beam. The double tapered cavity provides uniform strain distribution on the surface of the beam over its length hence the piezoelectric ceramic patches are bonded on the top surface of the beam. One piezoelectric patch is bonded exactly above the first tapered cavity from the fixed end and the second piezoelectric patch is placed above the second tapered cavity. The use of two piezoelectric patches helps to improve the amplitude of the harvested voltage over the operating frequency range (broadband) achieved by varying the overhang length. The performance of the proposed energy harvester is demonstrated by exciting the harvester with an electromagnetic exciter placed at the free end of the beam.

3. Modeling

The analytical model of the piezoelectric energy harvester designed using propped cantilever beam having double tapered cavity with variable overhang length shown in Fig. 1 is developed using Euler Bernoulli beam theory. For modeling, the energy harvester is split into five sections namely section I, II, III, IV and V as shown in Fig. 1. The sections I, IV and V consist of only regular beam element and sections

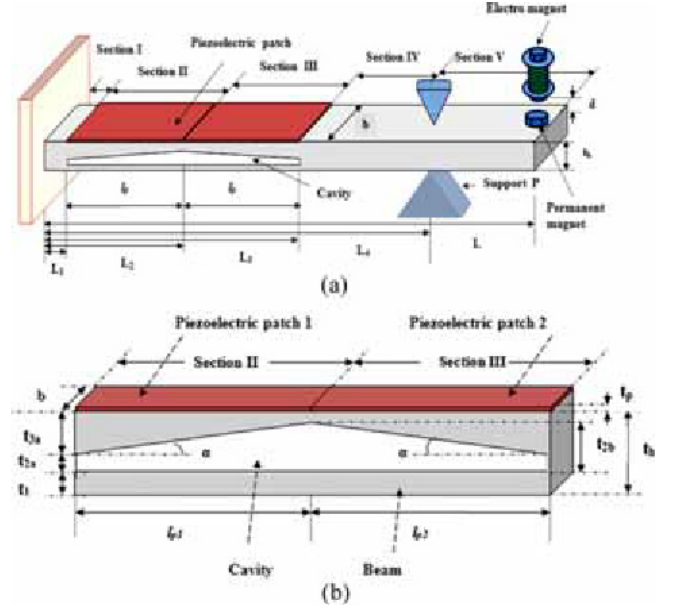


Fig. 1 Schematic of the Propped cantilever based piezoelectric energy harvester (a) with double tapered cavity (b) sections showing the double tapered cavity

II and III (composite sections) consist of beam with tapered cavity and a piezoelectric patch. The composite section shown in Fig. 1(b) consists of four layers namely, layer 1 with the thickness of t_1 (layer between the bottom surface of the beam and the bottom surface of the cavity), layer 2 with the thickness of $t_2(x)$ (double tapered cavity between layer 1 and layer 3), layer 3 with the thickness of $t_3(x)$ (beam layer between the cavity and the top surface of the beam) and layer 4 is the piezoelectric patch with the thickness of t_p .

The vibration governing equation of motion for all the sections of the energy harvester in Fig. 1 is given as Ref. 22.

$$\frac{d^4 W_n(x)}{dx^4} - \beta_n^4 W_n(x) = 0 \quad (L_{n-1} < x < L_n) \quad (1)$$

where $\beta_n^4 = \frac{\omega^2 m_n}{(EI)_n}$, $n = 1, 2, \dots, 5$, $L_0 = 0$, $L_5 = L$,

$W_n(x)$ is the amplitude of modal functions of the beam, ω is resonant angular frequency. As sections I, IV and V have only beam element with uniform dimensions, the flexural rigidity $(EI)_i$ and the mass per unit length m_i are constant and are given by

$$(EI)_i = E_b I_b \cdot m_i = \rho b t_b \quad (2)$$

where $I_b = \frac{b t_b^3}{12}$, $i = 1, 4, 5$

E_b , ρ_b , b and t_b are the Young's modulus, density, width and thickness of the beam. I_b is the moment of inertia corresponding to sections I, IV and V.

The flexural rigidity $(EI)_j$, where $j = 2, 3$ and the mass per unit length m_j , for sections II, III with double tapered cavity varies with the moment of inertia and thickness and are given by

$$(EI)_j = E_b [I_1(x) + I_3(x)] + E_p I_p(x) \\ m_j = b \{ \rho_b [t_1 + t_3(x)] + \rho_p t_p \} \quad (3)$$

$$\text{where, } I_1(x) = \frac{bt_1^3}{12} + bt_1(Y_{NA}(x) - y_1)^2$$

$$I_3(x) = \frac{bt_3^3(x)}{12} + bt_3(x)(Y_{NA}(x) - y_3(x))^2$$

$$I_p(x) = \frac{bt_p^3}{12} + bt_p(Y_{NA}(x) - y_p)^2$$

$$\text{with } y_1 = \frac{t_1}{2}, y_3(x) = \frac{t_3(x)}{2} + t_2(x) + t_1, y_p = \frac{t_p}{2} + t_b$$

$$Y_{NA}(x) = \frac{E_b\{0.5t_1^2 + t_3(x)[0.5t_3(x) + t_2(x) + t_1]\} + E_p t_p(0.5t_p + t_b)}{E_b[t_1 + t_3(x)] + E_p t_p}$$

$$t_3(x) = t_b - t_1 - t_2(x),$$

$$t_2(x) = t_{2a} + \alpha x \quad (0 \leq x \leq l_{p1})$$

$$t_2(x) = t_{2b} - \alpha x \quad (l_{p1} \leq x \leq l_{p2})$$

$$\alpha = \frac{t_{2b} - t_{2a}}{l_p} \quad (l_{p1} = l_{p2} = l_p)$$

where E_p , ρ_p , b and t_p are the Young's modulus, density, width and thickness of the piezoelectric patch. $I_1(x)$, $I_3(x)$ and $I_p(x)$ are the moment of inertia of layer 1, layer 3 and the piezoelectric layer, t_1 , $t_2(x)$ and $t_3(x)$ are the thickness of layer 1, layer 2 and layer 3 of section II and III. ' α ' is the taper angle, t_{2a} , t_{2b} , are the thickness of the smaller and wider side of the tapered cavity as shown in Fig. 1b y_1 , y_3 are the neutral axis of layer 1 and layer 3. $Y_{NA}(x)$ is the location of neutral axis of the composite section. l_{p1} , l_{p2} , are the length of piezoelectric patch 1 and 2 respectively.

The free vibration solution for Eq. (1) is given by

$$W_n(x) = A_n \sin \beta_n x + B_n \cos \beta_n x + C_n \sinh \beta_n x + D_n \cosh \beta_n x \quad (4)$$

where $\beta_n^4 = \frac{\omega^2 m_n}{(EI)_n}$ and A_n , B_n , C_n and D_n are the constants of integration obtained by substituting the following boundary and the continuity conditions. The boundary conditions are Ref. 23

$$\text{At } x = 0 \quad W_1(0) = 0, \quad \frac{dW_1(0)}{dx} = 0$$

$$\text{At } x = L \quad \frac{d^2 W_5(L)}{dx^2} = 0, \quad \frac{d^3 W_5(L)}{dx^3} = 0$$

The continuity conditions at $x = L_q$, where $q = 1, 2, 3$ are

$$W_q(L_q) = W_{q+1}(L_q), \quad \frac{dW_q(L_q)}{dx} = \frac{dW_{q+1}(L_q)}{dx} \quad (5)$$

$$(EI)_q \frac{d^2 W_q(L_q)}{dx^2} = (EI)_{q+1} \frac{d^2 W_{q+1}(L_q)}{dx^2} + M_e$$

$$(EI)_q \frac{d^3 W_q(L_q)}{dx^3} = (EI)_{q+1} \frac{d^3 W_{q+1}(L_q)}{dx^3}$$

The continuity conditions at the support $x = L_4$ are Ref. 24.

$$W_4(L_4) = W_5(L_4) = 0, \quad \frac{dW_4(L_4)}{dx} = \frac{dW_5(L_4)}{dx}$$

$$(EI)_4 \frac{d^2 W_4(L_4)}{dx^2} = (EI)_5 \frac{d^2 W_5(L_4)}{dx^2}$$

where $M_e = S \frac{t_b - t_p}{2}$ is the bending moment induced at the two ends of the piezoelectric patch $S = \frac{E_b t_b b}{\phi + \gamma} d_{31} \frac{V_g}{t_p}$ is the shear force generated at the interface between the piezoelectric patch and the host beam, $\phi = \frac{E_b t_b}{E_p t_p}$, d_{31} is the piezoelectric charge coefficient, V_g is the voltage generated from the piezoelectric patch and $\gamma = 6,^{23}$ when a bending beam is considered.

Applying boundary and continuity conditions in Eq. (4), the coefficients A_n , B_n , C_n , D_n are obtained by solving the Eigen value problem. Setting the determinant of the characteristics matrix

$$K(\beta) = 0 \quad (6)$$

where $K(\beta)$ is a 20×20 matrix, the β values and the natural frequencies for all modes can be obtained.

The forced vibration solution of the beam due to dynamic force $f(x, t) = F \sin(\omega' t) \delta(x - L)$ applied at its free end is expressed as²³

$$Y_{1,2,\dots,5}(x, t) = W_{1,2,\dots,5}(x) \frac{FW(L) \sin(\omega' t)}{\int_0^L W_{1-5}(x) dx (\omega_n^2 - \omega'^2)} \quad (7)$$

where $W_{1,2,\dots,5} = \sum W_j(x)$ is the transverse displacement of the beam, $i = 1, 2, 5$, $L_0^j = 0$, $L_i = L$, x is the position on the beam ($0 \leq x \leq L$), $\delta(x - L)$ is the Dirac delta function to model point force and F , ω are the magnitude and angular frequency of input vibration force respectively.

The magnitude of the dynamic force F at the free end of the beam²⁵ is given by,

$$F = \frac{N_c I A B_p}{2L_e} \left(\frac{L_q + d}{\sqrt{R^2 + (L_p + d)^2}} - \frac{d}{\sqrt{R^2 + d^2}} \right) \quad (8)$$

where N_c is number of coil turns, I is magnitude of current given to coil, A is the cross sectional area of core, B_p is the flux density of the permanent magnet, L_e is the length of the electromagnet, L_p is the length of the permanent magnet, R is the radius of the permanent magnet and d is the gap between the magnets as shown in Fig. 1.

The generated voltage from the piezoelectric patch1 and patch 2 bonded on the beam subjected to the dynamic loading can be solved as Ref. 23.

$$V_1(t) = Z_g(x) \left(\frac{dW_2(x)}{dx} \Big|_{x=L_2} - \frac{dW_2(x)}{dx} \Big|_{x=L_1} \right) \sin(\omega' t)$$

$$V_2(t) = Z_g(x) \left(\frac{dW_3(x)}{dx} \Big|_{x=L_3} - \frac{dW_3(x)}{dx} \Big|_{x=L_2} \right) \sin(\omega' t) \quad (9)$$

$$\text{where } Z_g(x) = \frac{e_{31} y_c b}{C_v} \frac{FW_5(L)}{\int_0^L W_{1-5}(x) dx (\omega^2 - \omega'^2)}$$

$$y_c = t_b + 0.5t_p - \frac{E_b[3t_1 t_{2a} + 3(t_1 + t_{2a})(t_{3a} + t_{3b}) + t_{3a}^2 + t_{3b}^2 + t_{3a} t_{3b}] + 6E_p t_p(t + 0.5t_p)}{E_b[6t_1 + 3(t_{3a} + t_{3b})] + 6E_p t_p}$$

where e_{31} is the piezoelectric constant, C_v is the electrical capacity of the piezoelectric patch. y_c is the perpendicular distance from the beam neutral axis (Y_{NA}) and the middle of the piezoelectric element for section II and III.^{26,27} The maximum value of power generated from the

energy harvester (P_g) is given by Ref. 28

$$P_g = \frac{V_g^2}{R_L} \quad (10)$$

where, V_g is the maximum value of the generated voltage. The optimum load resistance (R_L) of the energy harvester at the open circuit fundamental natural frequency is given by Ref. 29.

$$R_L = \frac{1}{\omega C_v} \left[\frac{1 - \zeta^2 + (\gamma/2\zeta)^2}{(1 + \gamma - \zeta^2)(1 + \gamma - 2\zeta^2)} \right]^{\frac{1}{2}} \quad (11)$$

where ζ is the damping ratio $\zeta = \frac{(B^2 - 4AC)^{\frac{1}{2}} - B}{2A}$, A, B and C are coefficients. $A = 4(1 + \nu^2)$, $B = 4\gamma\nu$

$C = \nu^2 \gamma^2 - \left(\frac{\gamma\nu\sigma}{|\alpha(1)|\tilde{\theta}} \right)^2$ The dimensionless terms are given by

$\nu = R_L C_v \omega$, $\gamma = \frac{\tilde{\theta}}{C_v \omega^2}$, $\sigma = \frac{\cosh \lambda - \cos \lambda}{\sinh \lambda - \sin \lambda}$ and the values of λ changes with the position of the support P.

$|\tilde{\alpha}(1)| = \frac{\gamma\nu|\sigma|\tilde{\theta}}{[(2\nu\zeta)^2 + (2\zeta + \nu\gamma)^2]^{\frac{1}{2}}}$ where $\tilde{\theta}$ is the electromechanical coupling given by

$$\tilde{\theta} = -e_{31} b y_c \left(\frac{dW_2(x)}{dx} \Big|_{x=L_2} - \frac{dW_2(x)}{dx} \Big|_{x=L_1} \right)$$

4. Results of Theoretical Analysis

The performance of the energy harvester is evaluated from the model derived in Section 3 through simulation. The variation in the first mode frequencies of the harvester having taper angle $\alpha = 0^\circ$, $\alpha = 0.75^\circ$, $\alpha = 1.5^\circ$, $\alpha = 2.25^\circ$ for different position of the support P and for the beam without cavity obtained is shown in Fig. 2. The results reveal that the first mode frequency is found to increase linearly with the position of the support P up to $0.783 L$ from fixed end. It can also be observed that with the increase in taper angle from $\alpha = 0^\circ$ to $\alpha = 2.25^\circ$, the mode frequency is found to decrease, however the magnitude of reduction in frequency is very small. Further from the theoretical analysis the second and third mode frequencies with variation in support position are found to be non linear.

The mode shape for the first natural frequency when the support P is placed at a distance of $x = 0.4 L$ and $x = 0.6 L$ from the fixed end is shown in Fig. 3. The results show that the tip deflection for the first mode frequency increases with the taper angle and decreases when the support is placed away from the fixed end. Also the tip deflection with double tapered cavity for any position of support P is higher, as compared to the beam without cavity. The theoretical analysis also inferred that the tip deflection for any position of support P for second and third mode is found to be small in magnitude. For the reasons mentioned above, the second and third mode frequencies are not considered for designing the broadband energy harvester in this work.

The voltage generated from the energy harvester for the positional variation of support P from $x = 0.38 L$ to $x = 0.64 L$ from the fixed end and the output voltage generated for the frequency corresponds to that

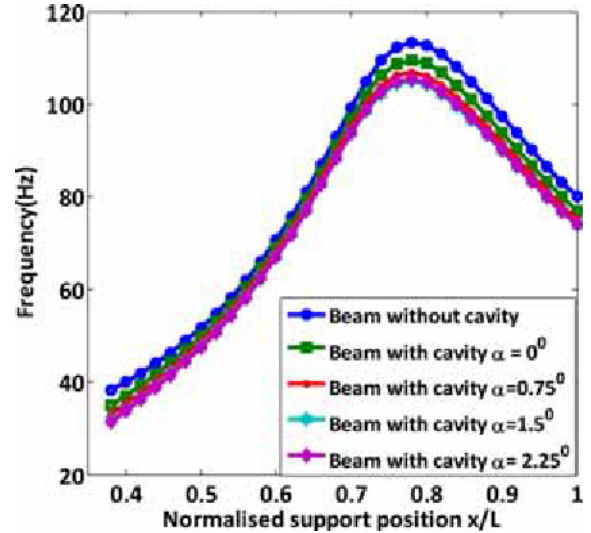


Fig. 2 First mode frequency

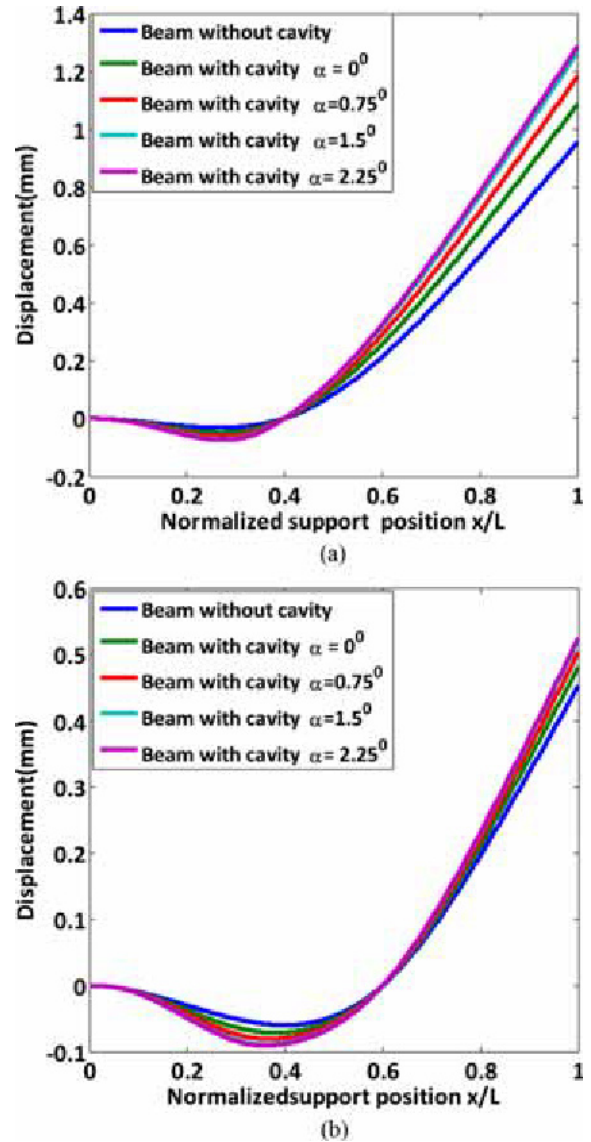


Fig. 3 First mode shape when the support P is at (a) $x = 0.4 L$ (b) $x = 0.6 L$

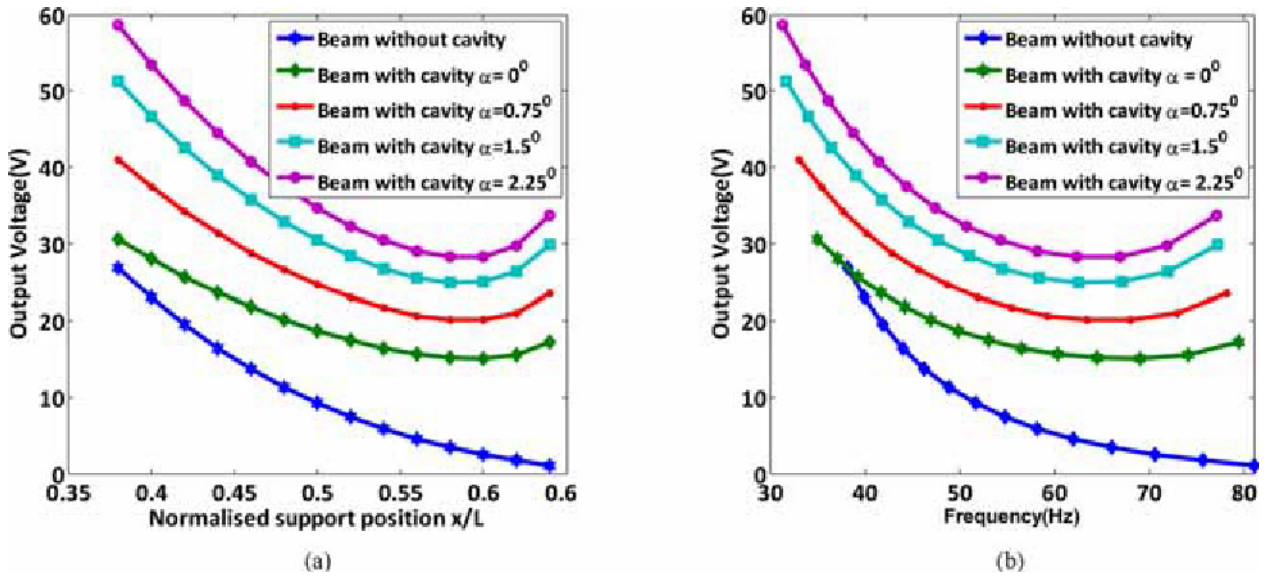


Fig. 4 Voltage generated from the energy harvester: (a) With variation in support position, (b) With variation in frequency with frequency

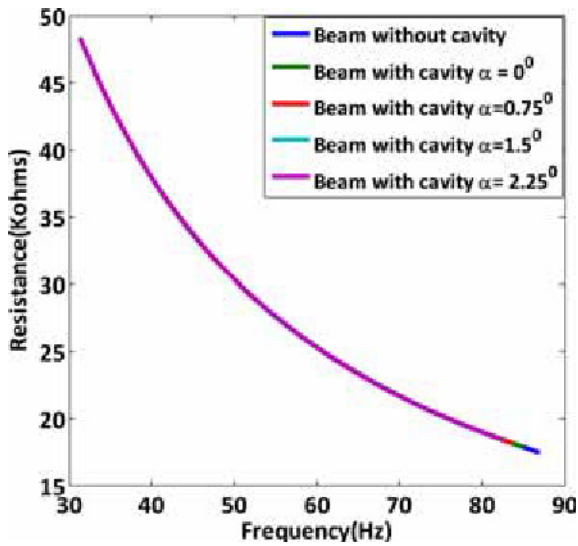


Fig. 5 Variation in the load resistance

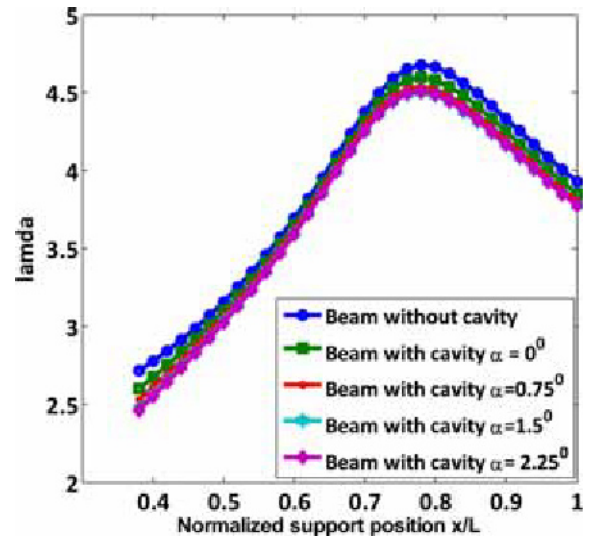


Fig. 6 Variation in weighted frequency (λ) with support position

Table 1 Range of bandwidth, voltage generated and harvested power

Energy harvester configuration	Operating frequency range	Bandwidth(Hz)	Output voltage range	Harvested power range	
Beam without cavity	38.2 Hz - 81.07 Hz	42.87	26.9 V - 1.03 V	18.23 mW - 0.056 mW	
Beam with double tapered cavity having taper angle α	$\alpha = 0^\circ$	34.98 Hz - 79.38 Hz	44.41	30.6 V - 17.17 V	21.41 mW - 15.45 mW
	$\alpha = 0.75^\circ$	33.08 Hz - 78.14 Hz	45.06	41.03 V - 23.49 V	35.78 mW - 28.46 mW
	$\alpha = 1.5^\circ$	31.68 Hz - 77.17 Hz	45.49	51.23 V - 29.89 V	52.11 mW - 45.5 mW
	$\alpha = 2.25^\circ$	31.35 Hz - 77.08 Hz	45.73	58.6 V - 33.7 V	71.02 mW - 57.74 mW

position of support P are given in Fig. 4. The generated voltage and the harvested power from the energy harvesters in the operating frequency range are summarized in Table 1. The results show that the double tapered cavity in the energy harvester enhances the magnitude of the generated voltage range in large extent as compared to that of the harvester designed without cavity. And also it is observed that the cavity provides a meager improvement in the operating frequency range. The enhancement in the generated voltage is due to the enhanced strain distribution on the surface of the beam provided by the double tapered cavity.

The power P_g in Eq. (10) depends on the load resistance R_L which in turn depends on the mode frequency (ω) as given in Eq. (11), also the mode frequency (ω) and weighted frequency (λ) varies with the support position P. The results in Fig. 5 show the variation in the load resistance with the frequency. The variation in the weighted frequency (λ) with the support position is shown in Fig. 6. In the propped cantilever beam the weighted frequency (λ) varies with the position of support P. But in the case of cantilever beam, weighted frequency (λ) is constant. As the load resistance (R_L) given in Eq. (11) depends on λ , the power harvested also depends on λ .

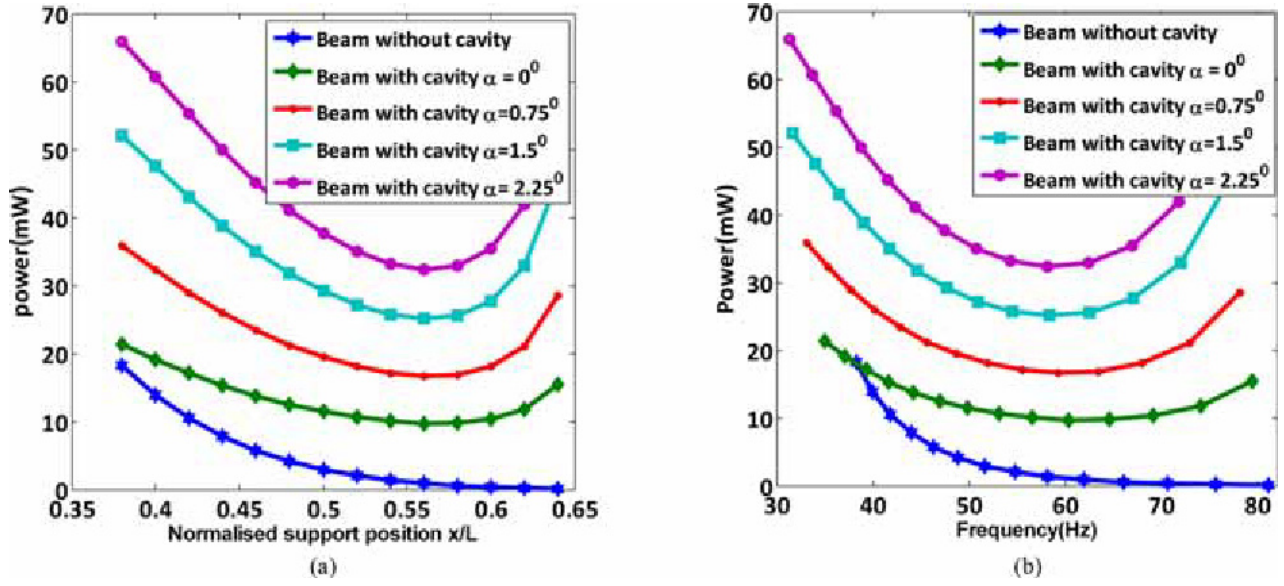


Fig. 7 Variation in harvested power: (a) With support position, (b) With frequency

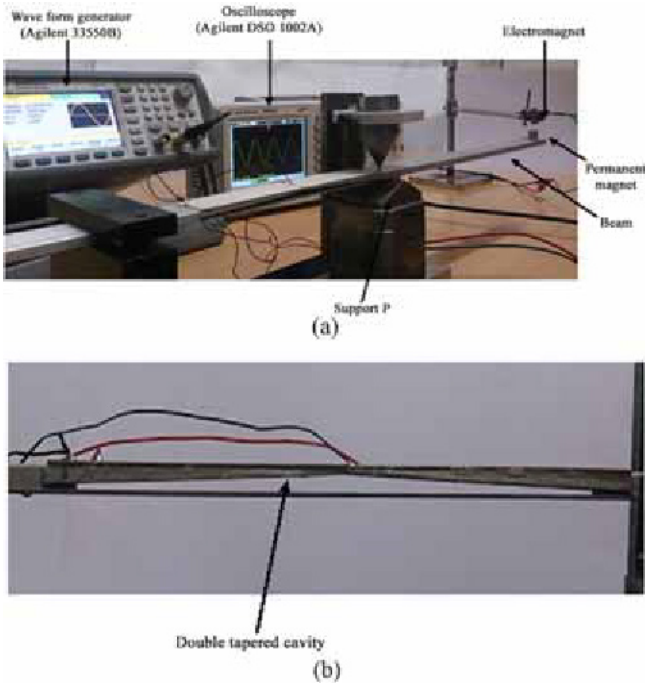


Fig. 8 Photograph of the fabricated broadband energy harvester with enhanced output: (a) Harvester with double tapered cavity, (b) View of double tapered cavity

The power harvested from the energy harvester computed using Eq. (10) is shown in Figs. 7(a) and 7(b). The enhanced strain due to the double tapered cavity in a propped cantilever beam, tends to decrease slightly as the pinned support moves away from the fixed end, hence there is a negative trend in the voltage and power harvested. When the support P, is placed at position $0.783 L$, the resonance frequency of the propped cantilever beam matches with the second mode frequency of the normal cantilever beam. The discrepancy between the analytical and experimental results in Fig. 9 is due to the variation in the moment of inertia along the length of the beam in section II and section III.

Table 2 Dimension and properties of aluminium beam

Symbol	Description	Value	Units
L	Length	500	mm
b	Width	25	mm
t_b	Thickness	5.5	mm
E_b	Young's modulus	71	GPa
ρ_b	Density	2700	Kgm ⁻³

Table 3 Dimension and properties of piezoelectric element (PZT 5H)

Symbol	Description	Value	Units
l_p	Length	76.5	mm
b_p	Width	25	mm
t_p	Thickness	0.5	mm
E_p	Young's modulus	47.62	GPa
ρ_p	Density	7500	Kgm ⁻³
e_{31}	Piezoelectric constant	-16.6	Cm ⁻²
d_{31}	Piezoelectric charge coefficient	-274	pCN ⁻¹
C_v	Capacitance	104.3	nF

5. Experimentation and Results

The energy harvester with the taper angle of $\alpha = 2.25^\circ$ ($t_{2a} = 1$ mm, $t_{2b} = 4$ mm), is fabricated for experimental investigation, as this configuration provides maximum voltage as shown in Table 1. The double tapered cavity is formed at a distance of $L_1 = 30$ mm from the fixed end and the photograph of the experimental set up is shown in Fig. 8. The double tapered cavity in the beam is shaped by wire cut EDM (Electric Discharge Machining) tool. The dimensions and the properties of the beam and the piezoelectric patch are given in Table 2 and 3. The specifications of electromagnetic excitation placed at the tip of the beam are: number of coil turns $N_c = 2000$, length $L_c = 16$ mm and cross sectional area $A = 78$ mm², flux density of the cylindrical permanent magnet $B_p = 1.1$ T, length $L_p = 10$ mm, radius $R = 5$ mm and the gap between the magnets $d = 6$ mm. The generated voltage from the energy harvester at resonance is measured experimentally for different

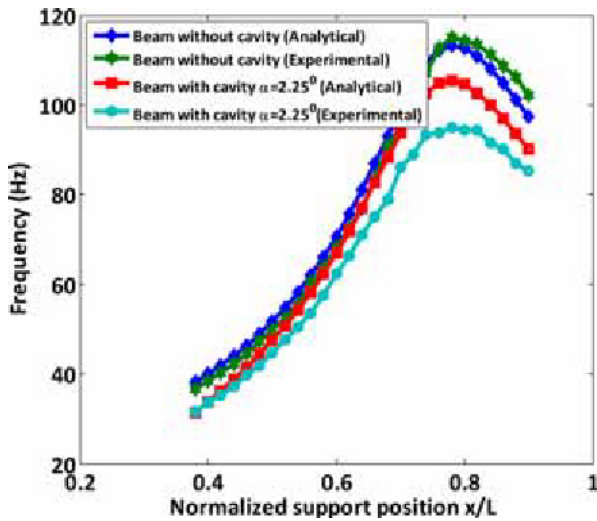
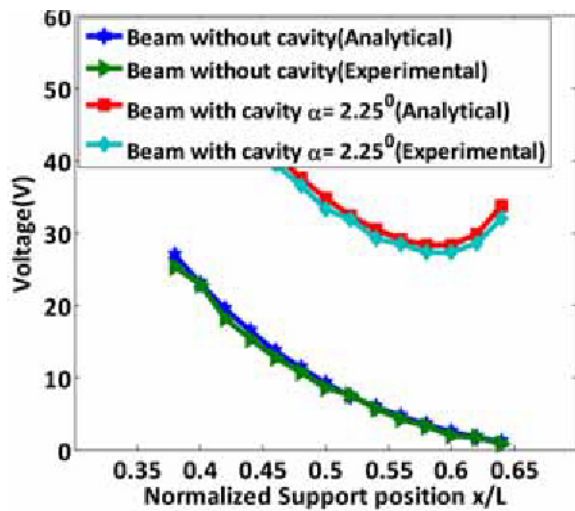
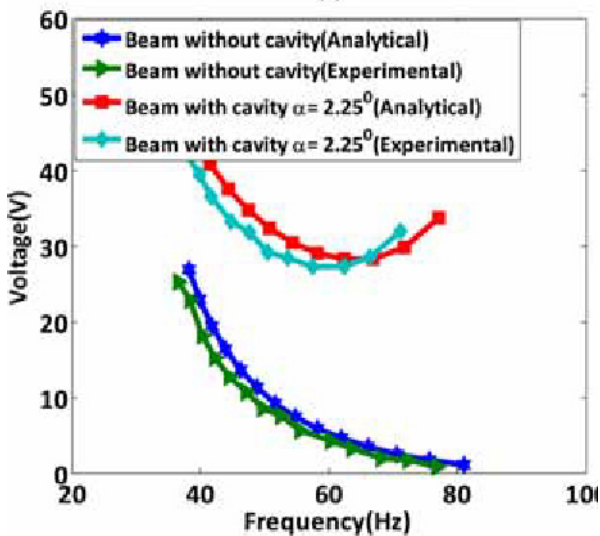


Fig. 9 First mode frequency of the energy harvester (Experimental and analytical)

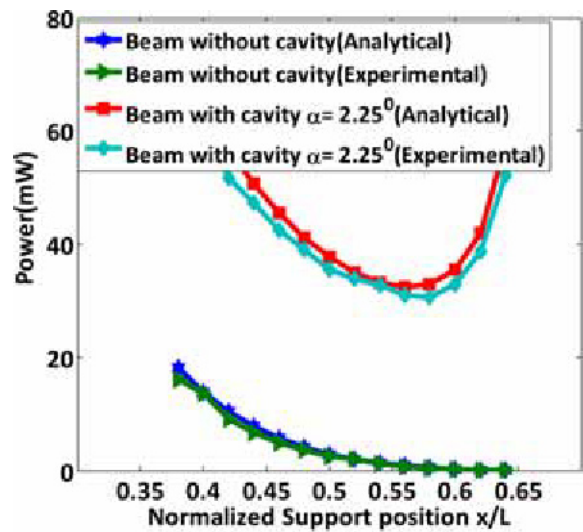


(a)

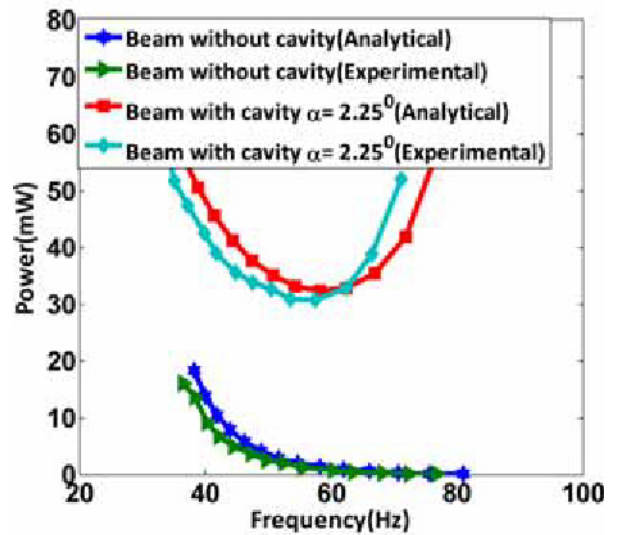


(b)

Fig. 10 Voltage generated from the energy harvester (Experimental and analytical): (a) With variation in support position, (b) With variation in frequency



(a)



(b)

Fig. 11 Variation in Harvested power from the energy harvester (Experimental and analytical): (a) With support position, (b) With frequency

position of the support P between $x = 0.38 L$ and $x = 0.64 L$ from the fixed end, by connecting the two piezoelectric patches in series. During experimentation in the laboratory for each position of the support P, the harvester is made to vibrate at resonance by tuning the excitation frequency of the electromagnetic exciter to the first mode frequency corresponds to that position. The amplitude of the excitation signal applied from the arbitrary waveform generator (Agilent 33500B) to the exciter is fixed as 10 V peak to peak for all position of support P and the generated voltage is measured using the digital storage oscilloscope (Agilent DSO 1002A).

The variation in the first mode frequency for different position of the support P measured in experimentation is shown in Fig. 9.

The voltage and power measured for different position of support P and its variation with frequency are shown in Figs. 10 and 11. The results shown in Figs. 9-11 are in close agreement with the result obtained from theoretical analysis for the harvester having taper angle

of $\alpha = 2.25^\circ$. The results show that the harvester with the cavity provides large enhancement in the amplitude of generated voltage in the operating frequency range.

6. Conclusions

A piezoelectric broadband energy harvester using propped cantilever beam having double tapered cavity with variable overhang length is designed, analytically modeled using Euler Bernoulli beam theory. Results from the analytical model reveal that the mode frequency is a function of the position of the support in the propped cantilever and the change in the mode frequency is found to be linear for the fundamental mode and non linear for the higher modes of vibration. The results infer that the operating the harvester in first mode frequency provides wider operating frequency range from 31.4 Hz to 105.4 Hz (broadband), which depends on position of the support. Further the results and analysis from the model reveal that the double tapered cavity and its variation in taper angle improves the amplitude of the generated voltage in large extent. The experimentation was conducted on the energy harvester having double tapered cavity with the taper angle $\alpha = 2.25^\circ$ and the results are in close agreement with the analytical results. The proposed broadband energy harvester is simple in design and generates enhanced output voltage in the operating frequency range. Moreover the harvester provides continuously and gradually varying output voltage in the operating frequency range as compared to the broadband energy harvesters proposed in the literature, which provides oscillatory output in the operating frequency range. Though the proposed harvester is designed with propped cantilever beam with variable overhang length, the boundary and continuity conditions requires only few modifications in the regular cantilever based piezoelectric energy harvester. The harvester proposed here can be used to power wireless sensor networks and low power electronic devices such as Bluetooth transceiver and palm MP3.

REFERENCES

- Kim, H. S., Kim, J.-H., and Kim, J., "A Review of Piezoelectric Energy Harvesting Based on Vibration," *Int. J. Precis. Eng. Manuf.*, Vol. 12, No. 6, pp. 1129-1141, 2011.
- Anton, S. R. and Sodano, H. A., "A Review of Power Harvesting Using Piezoelectric Materials (2003-2006)," *Smart Materials and Structures*, Vol. 16, No. 3, pp. R1-R21, 2007.
- Kim, J. E., Kim, H., Yoon, H., Kim, Y. Y., and Youn, B. D., "An Energy Conversion Model for Cantilevered Piezoelectric Vibration Energy Harvesters Using Only Measurable Parameters," *Int. J. Precis. Eng. Manuf.-Green Tech.*, Vol. 2, No. 1, pp. 51-57, 2015.
- Zhu, D., Tudor, M. J., and Beeby, S. P., "Strategies for Increasing the Operating Frequency Range of Vibration Energy Harvesters: A Review," *Measurement Science and Technology*, Vol. 21, No. 2, Paper No. 022001, 2009.
- Tang, L., Yang, Y., and Soh, C. K., "Toward Broadband Vibration-Based Energy Harvesting," *Journal of Intelligent Material Systems and Structures*, Vol. 21, No. 18, pp. 1867-1897, 2010.
- Shahruz, S., "Design of Mechanical Band-Pass Filters for Energy Scavenging: Multi-Degree-of-Freedom Models," *Journal of Vibration and Control*, Vol. 14, No. 5, pp. 753-768, 2008.
- Xue, H., Hu, Y., and Wang, Q.-M., "Broadband Piezoelectric Energy Harvesting Devices Using Multiple Bimorphs with Different Operating Frequencies," *IEEE Transactions on Ultrasonics, Ferroelectrics, and Frequency Control*, Vol. 55, No. 9, pp. 2104-2108, 2008.
- Ou, Q., Chen, X., Gutschmidt, S., Wood, A., Leigh, N., et al., "An Experimentally Validated Double-Mass Piezoelectric Cantilever Model for Broadband Vibration-Based Energy Harvesting," *Journal of Intelligent Material Systems and Structures*, Vol. 23, No. 2, pp. 117-126, 2012.
- Erturk, A., Renno, J. M., and Inman, D. J., "Modeling of Piezoelectric Energy Harvesting from an L Shaped Beam Mass Structure with an Application to UAVs," *Journal of Intelligent Material Systems and Structures*, Vol. 20, pp. 529-544, 2009.
- Yang, Z. and Yang, J., "Connected Vibrating Piezoelectric Bimorph Beams as a Wide-Band Piezoelectric Power Harvester," *Journal of Intelligent Material Systems and Structures*, Vol. 20, No. 5, pp. 569-574, 2009.
- Su, W.-J., Zu, J., and Zhu, Y., "Design and Development of a Broadband Magnet-Induced Dual-Cantilever Piezoelectric Energy Harvester," *Journal of Intelligent Material Systems and Structures*, DOI No. 10.1177/1045389X13498315, 2013.
- Zhou, W., Penamalli, G. R., and Zuo, L., "An Efficient Vibration Energy Harvester with a Multi-Mode Dynamic Magnifier," *Smart Materials and Structures*, Vol. 21, No. 1, Paper No. 015014, 2011.
- Wu, H., Tang, L., Yang, Y., and Soh, C. K., "A Novel Two-Degrees-of-Freedom Piezoelectric Energy Harvester," *Journal of Intelligent Material Systems and Structures*, DOI No. 10.1177/1045389X12457254, 2012.
- Niri, E. D. and Salamone, S., "A Passively Tunable Mechanism for a Dual Bimorph Energy Harvester with Variable Tip Stiffness and Axial Load," *Smart Materials and Structures*, Vol. 21, No. 12, Paper No. 125025, 2012.
- Zhu, Y., Zu, J., and Su, W., "Broadband Energy Harvesting through a Piezoelectric Beam Subjected to Dynamic Compressive Loading," *Smart Materials and Structures*, Vol. 22, No. 4, Paper No. 045007, 2013.
- Qi, S., Shuttleworth, R., Oyadiji, S. O., and Wright, J., "Design of a Multiresonant Beam for Broadband Piezoelectric Energy Harvesting," *Smart Materials and Structures*, Vol. 19, No. 9, Paper No. 094009, 2010.
- Kim, I.-H., Jung, H.-J., Lee, B. M., and Jang, S.-J., "Broadband Energy-Harvesting Using a Two Degree-of-Freedom Vibrating Body," *Applied Physics Letters*, Vol. 98, No. 21, Paper No. 214102, 2011.

18. Li, P., Liu, Y., Wang, Y., Luo, C., Li, G., et al., "Low-Frequency and Wideband Vibration Energy Harvester with Flexible Frame and Interdigital Structure," *AIP Advances*, Vol. 5, No. 4, Paper No. 047151, 2015.
19. Kumar, K. A., Ali, S., and Arockiarajan, A., "Piezomagnetoelastic Broadband Energy Harvester: Nonlinear Modeling and Characterization," *The European Physical Journal Special Topics*, Vol. 224, Nos. 14-15, pp. 2803-2822, 2015.
20. Singh, K. A., Kumar, R., and Weber, R. J., "A Broadband Bistable Piezoelectric Energy Harvester with Nonlinear High-Power Extraction," *IEEE Transactions on Power Electronics*, Vol. 30, No. 12, pp. 6763-6774, 2015.
21. Sang, C. M., Dayou, J., and Liew, W. Y., "Increasing the Output from Piezoelectric Energy Harvester Using Width-Split Method with Verification," *Int. J. Precis. Eng. Manuf.*, Vol. 14, No. 12, pp. 2149-2155, 2013.
22. Salehi-Khojin, A., Bashash, S., and Jalili, N., "Modeling and Experimental Vibration Analysis of Nanomechanical Cantilever Active Probes," *Journal of Micromechanics and Microengineering*, Vol. 18, No. 8, Paper No. 085008, 2008.
23. Wang, Q. and Wu, N., "Optimal Design of a Piezoelectric Coupled Beam for Power Harvesting," *Smart Materials and Structures*, Vol. 21, No. 8, Paper No. 085013, 2012.
24. Murphy, J. F., "Transverse Vibration of a Simply Supported Beam with Symmetric Overhang of Arbitrary Length," *Journal of Testing and Evaluation*, Vol. 25, No. 5, pp. 522-524, 1997.
25. Kumar, B. S., Suresh, K., Kumar, U. V., Uma, G., and Umapathy, M., "Resonance Based DC Current Sensor," *Measurement*, Vol. 45, No. 3, pp. 369-374, 2012.
26. Reddy, A. R., Umapathy, M., Ezhilarasi, D., and Uma, G., "Cantilever Beam with Trapezoidal Cavity for Improved Energy Harvesting," *Int. J. Precis. Eng. Manuf.*, Vol. 16, No. 8, pp. 1875-1881, 2015.
27. Reddy, A. R., Umapathy, M., Ezhilarasi, D., and Gandhi, U., "Improved Energy Harvesting from Vibration by Introducing Cavity in a Cantilever Beam," *Journal of Vibration and Control*, DOI No. 10.1177/1077546314558498, 2014.
28. Dai, H., Abdelkefi, A., and Wang, L., "Theoretical Modeling and Nonlinear Analysis of Piezoelectric Energy Harvesting from Vortex-Induced Vibrations," *Journal of Intelligent Material Systems and Structures*, Vol. 25, No. 14, pp. 1861-1874, 2014.
29. Erturk, A., "Electromechanical Modeling of Piezoelectric Energy Harvesters," Ph.D. Thesis, Engineering, Mechanics, Virginia Tech, 2009.